2

Digital Image Fundamentals

> Those who wish to succeed must ask the right preliminary questions.
>
> *Aristotle*

Preview

This chapter is an introduction to a number of basic concepts in digital image processing that are used throughout the book. Section 2.1 summarizes some important aspects of the human visual system, including image formation in the eye and its capabilities for brightness adaptation and discrimination. Section 2.2 discusses light, other components of the electromagnetic spectrum, and their imaging characteristics. Section 2.3 discusses imaging sensors and how they are used to generate digital images. Section 2.4 introduces the concepts of uniform image sampling and intensity quantization. Additional topics discussed in that section include digital image representation, the effects of varying the number of samples and intensity levels in an image, the concepts of spatial and intensity resolution, and the principles of image interpolation. Section 2.5 deals with a variety of basic relationships between pixels. Finally, Section 2.6 is an introduction to the principal mathematical tools we use throughout the book. A second objective of that section is to help you begin developing a "feel" for how these tools are used in a variety of basic image processing tasks.

Upon completion of this chapter, readers should:

- Have an understanding of some important functions and limitations of human vision.
- Be familiar with the electromagnetic energy spectrum, including basic properties of light.
- Know how digital images are generated and represented.
- Understand the basics of image sampling and quantization.
- Be familiar with spatial and intensity resolution and their effects on image appearance.
- Have an understanding of basic geometric relationships between image pixels.
- Be familiar with the principal mathematical tools used in digital image processing.
- Be able to apply a variety of introductory digital image processing techniques.

2.1 ELEMENTS OF VISUAL PERCEPTION

Although the field of digital image processing is built on a foundation of mathematics, human intuition and analysis often play a role in the choice of one technique versus another, and this choice often is made based on subjective, visual judgments. Thus, developing an understanding of basic characteristics of human visual perception as a first step in our journey through this book is appropriate. In particular, our interest is in the elementary mechanics of how images are formed and perceived by humans. We are interested in learning the physical limitations of human vision in terms of factors that also are used in our work with digital images. Factors such as how human and electronic imaging devices compare in terms of resolution and ability to adapt to changes in illumination are not only interesting, they are also important from a practical point of view.

STRUCTURE OF THE HUMAN EYE

Figure 2.1 shows a simplified cross section of the human eye. The eye is nearly a sphere (with a diameter of about 20 mm) enclosed by three membranes: the *cornea* and *sclera* outer cover; the *choroid*; and the *retina*. The cornea is a tough, transparent tissue that covers the anterior surface of the eye. Continuous with the cornea, the sclera is an opaque membrane that encloses the remainder of the optic globe.

The choroid lies directly below the sclera. This membrane contains a network of blood vessels that serve as the major source of nutrition to the eye. Even superficial

FIGURE 2.1
Simplified diagram of a cross section of the human eye.
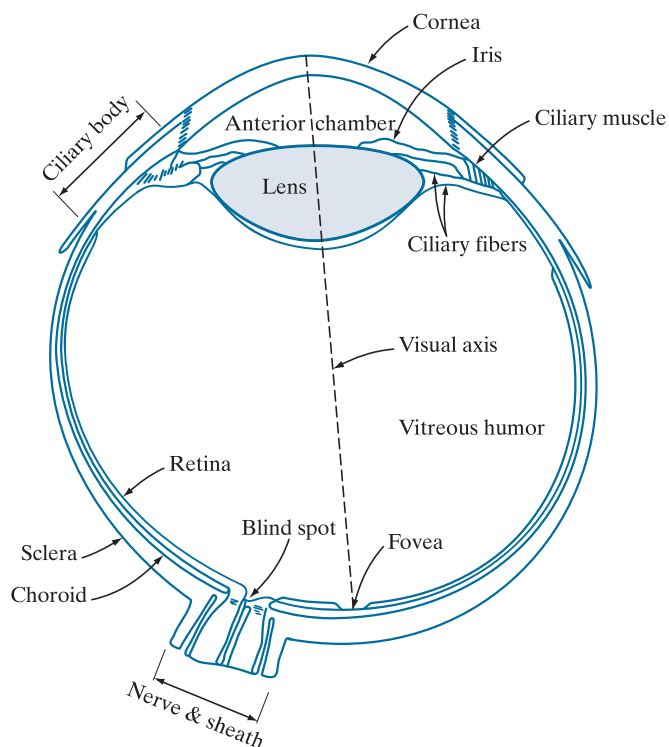
injury to the choroid can lead to severe eye damage as a result of inflammation that restricts blood flow. The choroid coat is heavily pigmented, which helps reduce the amount of extraneous light entering the eye and the backscatter within the optic globe. At its anterior extreme, the choroid is divided into the *ciliary body* and the *iris*. The latter contracts or expands to control the amount of light that enters the eye. The central opening of the iris (the *pupil*) varies in diameter from approximately 2 to 8 mm. The front of the iris contains the visible pigment of the eye, whereas the back contains a black pigment.

The *lens* consists of concentric layers of fibrous cells and is suspended by fibers that attach to the ciliary body. It is composed of 60% to 70% water, about 6% fat, and more protein than any other tissue in the eye. The lens is colored by a slightly yellow pigmentation that increases with age. In extreme cases, excessive clouding of the lens, referred to as *cataracts*, can lead to poor color discrimination and loss of clear vision. The lens absorbs approximately 8% of the visible light spectrum, with higher absorption at shorter wavelengths. Both infrared and ultraviolet light are absorbed by proteins within the lens and, in excessive amounts, can damage the eye.

The innermost membrane of the eye is the *retina*, which lines the inside of the wall's entire posterior portion. When the eye is focused, light from an object is imaged on the retina. Pattern vision is afforded by discrete light receptors distributed over the surface of the retina. There are two types of receptors: *cones* and *rods*. There are between 6 and 7 million cones in each eye. They are located primarily in the central portion of the retina, called the *fovea*, and are highly sensitive to color. Humans can resolve fine details because each cone is connected to its own nerve end. Muscles rotate the eye until the image of a region of interest falls on the fovea. Cone vision is called *photopic* or *bright-light* vision.

The number of rods is much larger: Some 75 to 150 million are distributed over the retina. The larger area of distribution, and the fact that several rods are connected to a single nerve ending, reduces the amount of detail discernible by these receptors. Rods capture an overall image of the field of view. They are not involved in color vision, and are sensitive to low levels of illumination. For example, objects that appear brightly colored in daylight appear as colorless forms in moonlight because only the rods are stimulated. This phenomenon is known as *scotopic* or *dim-light* vision.

Figure 2.2 shows the density of rods and cones for a cross section of the right eye, passing through the region where the optic nerve emerges from the eye. The absence of receptors in this area causes the so-called *blind spot* (see Fig. 2.1). Except for this region, the distribution of receptors is radially symmetric about the fovea. Receptor density is measured in degrees from the visual axis. Note in Fig. 2.2 that cones are most dense in the center area of the fovea, and that rods increase in density from the center out to approximately 20° off axis. Then, their density decreases out to the periphery of the retina.

The fovea itself is a circular indentation in the retina of about 1.5 mm in diameter, so it has an area of approximately 1.77 mm^2. As Fig. 2.2 shows, the density of cones in that area of the retina is on the order of 150,000 elements per mm^2. Based on these figures, the number of cones in the fovea, which is the region of highest acuity

FIGURE 2.2
Distribution of
rods and cones in
the retina.
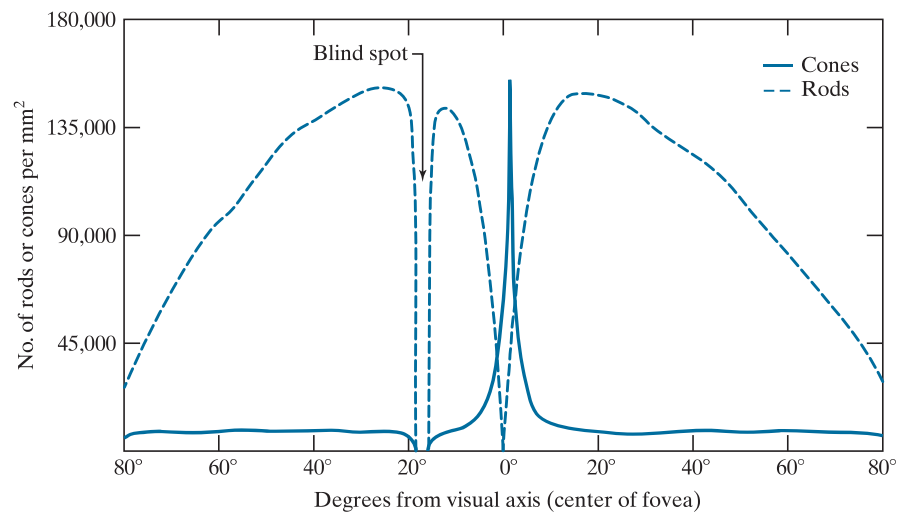
in the eye, is about 265,000 elements. Modern electronic imaging chips exceed this number by a large factor. While the ability of humans to integrate intelligence and experience with vision makes purely quantitative comparisons somewhat superficial, keep in mind for future discussions that electronic imaging sensors can easily exceed the capability of the eye in resolving image detail.

IMAGE FORMATION IN THE EYE

In an ordinary photographic camera, the lens has a fixed focal length. Focusing at various distances is achieved by varying the distance between the lens and the imaging plane, where the film (or imaging chip in the case of a digital camera) is located. In the human eye, the converse is true; the distance between the center of the lens and the imaging sensor (the retina) is fixed, and the focal length needed to achieve proper focus is obtained by varying the shape of the lens. The fibers in the ciliary body accomplish this by flattening or thickening the lens for distant or near objects, respectively. The distance between the center of the lens and the retina along the visual axis is approximately 17 mm. The range of focal lengths is approximately 14 mm to 17 mm, the latter taking place when the eye is relaxed and focused at distances greater than about 3 m. The geometry in Fig. 2.3 illustrates how to obtain the dimensions of an image formed on the retina. For example, suppose that a person is looking at a tree 15 m high at a distance of 100 m. Letting h denote the height of that object in the retinal image, the geometry of Fig. 2.3 yields $15/100 = h/17$ or $h = 2.5$ mm. As indicated earlier in this section, the retinal image is focused primarily on the region of the fovea. Perception then takes place by the relative excitation of light receptors, which transform radiant energy into electrical impulses that ultimately are decoded by the brain.

BRIGHTNESS ADAPTATION AND DISCRIMINATION

Because digital images are displayed as sets of discrete intensities, the eye's ability to discriminate between different intensity levels is an important consideration

FIGURE 2.3
Graphical representation of the eye looking at a palm tree. Point C is the focal center of the lens.
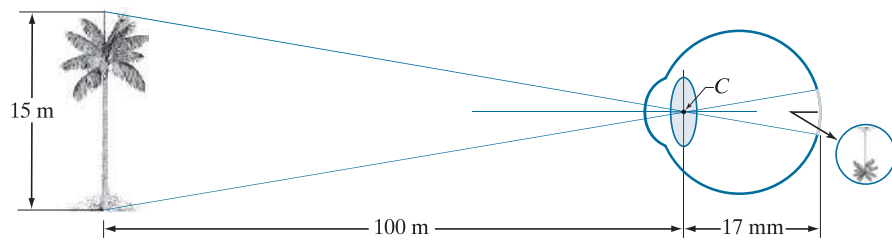
in presenting image processing results. The range of light intensity levels to which the human visual system can adapt is enormous—on the order of 10^{10}— from the scotopic threshold to the glare limit. Experimental evidence indicates that *subjective brightness* (intensity as perceived by the human visual system) is a logarithmic function of the light intensity incident on the eye. Figure 2.4, a plot of light intensity versus subjective brightness, illustrates this characteristic. The long solid curve represents the range of intensities to which the visual system can adapt. In photopic vision alone, the range is about 10^6. The transition from scotopic to photopic vision is gradual over the approximate range from 0.001 to 0.1 millilambert (−3 to −1 mL in the log scale), as the double branches of the adaptation curve in this range show.

The key point in interpreting the impressive dynamic range depicted in Fig. 2.4 is that the visual system cannot operate over such a range *simultaneously*. Rather, it accomplishes this large variation by changing its overall sensitivity, a phenomenon known as *brightness adaptation*. The total range of distinct intensity levels the eye can discriminate simultaneously is rather small when compared with the total adaptation range. For a given set of conditions, the current sensitivity level of the visual system is called the *brightness adaptation level*, which may correspond, for example,

FIGURE 2.4
Range of subjective brightness sensations showing a particular adaptation level, B_a.
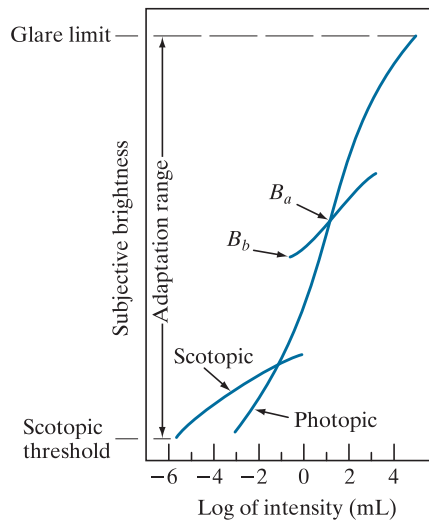
to brightness B_a in Fig. 2.4. The short intersecting curve represents the range of subjective brightness that the eye can perceive when adapted to *this* level. This range is rather restricted, having a level B_b at, and below which, all stimuli are perceived as indistinguishable blacks. The upper portion of the curve is not actually restricted but, if extended too far, loses its meaning because much higher intensities would simply raise the adaptation level higher than B_a.

The ability of the eye to discriminate between *changes* in light intensity at any specific adaptation level is of considerable interest. A classic experiment used to determine the capability of the human visual system for brightness discrimination consists of having a subject look at a flat, uniformly illuminated area large enough to occupy the entire field of view. This area typically is a diffuser, such as opaque glass, illuminated from behind by a light source, I, with variable intensity. To this field is added an increment of illumination, ΔI, in the form of a short-duration flash that appears as a circle in the center of the uniformly illuminated field, as Fig. 2.5 shows.

If ΔI is not bright enough, the subject says "no," indicating no perceivable change. As ΔI gets stronger, the subject may give a positive response of "yes," indicating a perceived change. Finally, when ΔI is strong enough, the subject will give a response of "yes" all the time. The quantity $\Delta I_c/I$, where ΔI_c is the increment of illumination discriminable 50% of the time with background illumination I, is called the *Weber ratio*. A small value of $\Delta I_c/I$ means that a small percentage change in intensity is discriminable. This represents "good" brightness discrimination. Conversely, a large value of $\Delta I_c/I$ means that a large percentage change in intensity is required for the eye to detect the change. This represents "poor" brightness discrimination.

A plot of $\Delta I_c/I$ as a function of $\log I$ has the characteristic shape shown in Fig. 2.6. This curve shows that brightness discrimination is poor (the Weber ratio is large) at low levels of illumination, and it improves significantly (the Weber ratio decreases) as background illumination increases. The two branches in the curve reflect the fact that at low levels of illumination vision is carried out by the rods, whereas, at high levels, vision is a function of cones.

If the background illumination is held constant and the intensity of the other source, instead of flashing, is now allowed to vary incrementally from never being perceived to always being perceived, the typical observer can discern a total of one to two dozen different intensity changes. Roughly, this result is related to the number of different intensities a person can see at any one *point* or *small area* in a monochrome image. This does not mean that an image can be represented by such a small number of intensity values because, as the eye roams about the image, the average

FIGURE 2.5
Basic experimental setup used to characterize brightness discrimination.
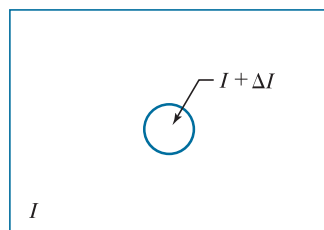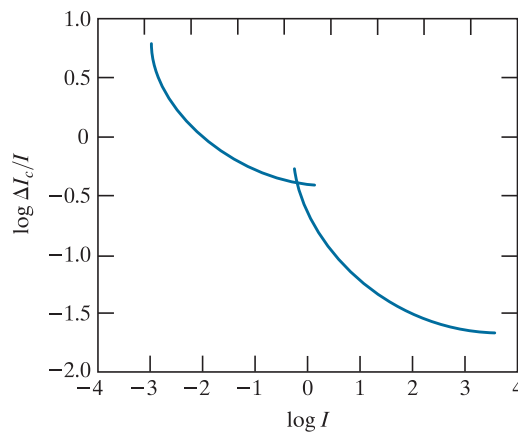
background changes, thus allowing a *different* set of incremental changes to be detected at each new adaptation level. The net result is that the eye is capable of a broader range of *overall* intensity discrimination. In fact, as we will show in Section 2.4, the eye is capable of detecting objectionable effects in monochrome images whose overall intensity is represented by fewer than approximately two dozen levels.

Two phenomena demonstrate that perceived brightness is not a simple function of intensity. The first is based on the fact that the visual system tends to undershoot or overshoot around the boundary of regions of different intensities. Figure 2.7(a) shows a striking example of this phenomenon. Although the intensity of the stripes

a
b
c

FIGURE 2.7
Illustration of the
Mach band effect.
Perceived
intensity is not a
simple function of
actual intensity.
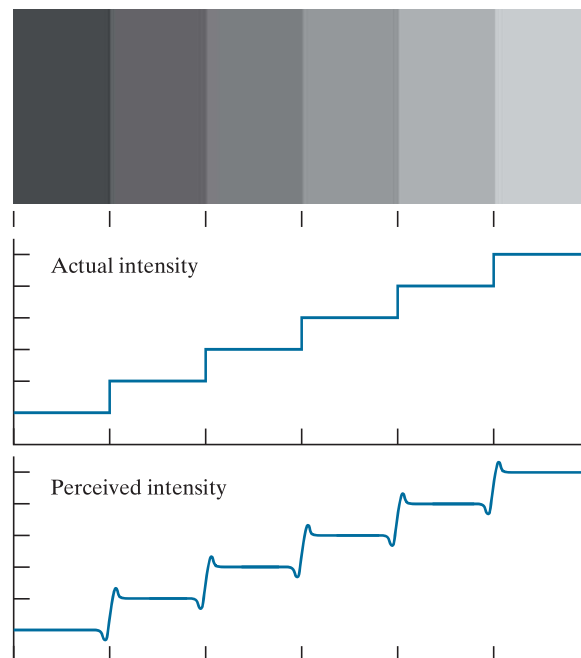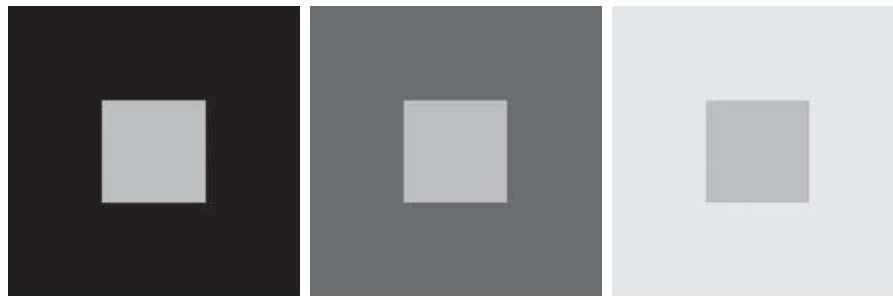
a b c

FIGURE 2.8 Examples of simultaneous contrast. All the inner squares have the same intensity, but they appear progressively darker as the background becomes lighter.

is constant [see Fig. 2.7(b)], we actually perceive a brightness pattern that is strongly scalloped near the boundaries, as Fig. 2.7(c) shows. These perceived scalloped bands are called *Mach bands* after Ernst Mach, who first described the phenomenon in 1865.

The second phenomenon, called *simultaneous contrast*, is that a region's perceived brightness does not depend only on its intensity, as Fig. 2.8 demonstrates. All the center squares have exactly the same intensity, but each appears to the eye to become darker as the background gets lighter. A more familiar example is a piece of paper that looks white when lying on a desk, but can appear totally black when used to shield the eyes while looking directly at a bright sky.

Other examples of human perception phenomena are *optical illusions*, in which the eye fills in nonexisting details or wrongly perceives geometrical properties of objects. Figure 2.9 shows some examples. In Fig. 2.9(a), the outline of a square is seen clearly, despite the fact that no lines defining such a figure are part of the image. The same effect, this time with a circle, can be seen in Fig. 2.9(b); note how just a few lines are sufficient to give the illusion of a complete circle. The two horizontal line segments in Fig. 2.9(c) are of the same length, but one appears shorter than the other. Finally, all long lines in Fig. 2.9(d) are equidistant and parallel. Yet, the crosshatching creates the illusion that those lines are far from being parallel.

2.2 LIGHT AND THE ELECTROMAGNETIC SPECTRUM

The electromagnetic spectrum was introduced in Section 1.3. We now consider this topic in more detail. In 1666, Sir Isaac Newton discovered that when a beam of sunlight passes through a glass prism, the emerging beam of light is not white but consists instead of a continuous spectrum of colors ranging from violet at one end to red at the other. As Fig. 2.10 shows, the range of colors we perceive in visible light is a small portion of the electromagnetic spectrum. On one end of the spectrum are radio waves with wavelengths billions of times longer than those of visible light. On the other end of the spectrum are gamma rays with wavelengths millions of times smaller than those of visible light. We showed examples in Section 1.3 of images in most of the bands in the EM spectrum.

a b
c d

FIGURE 2.9 Some well-known optical illusions.
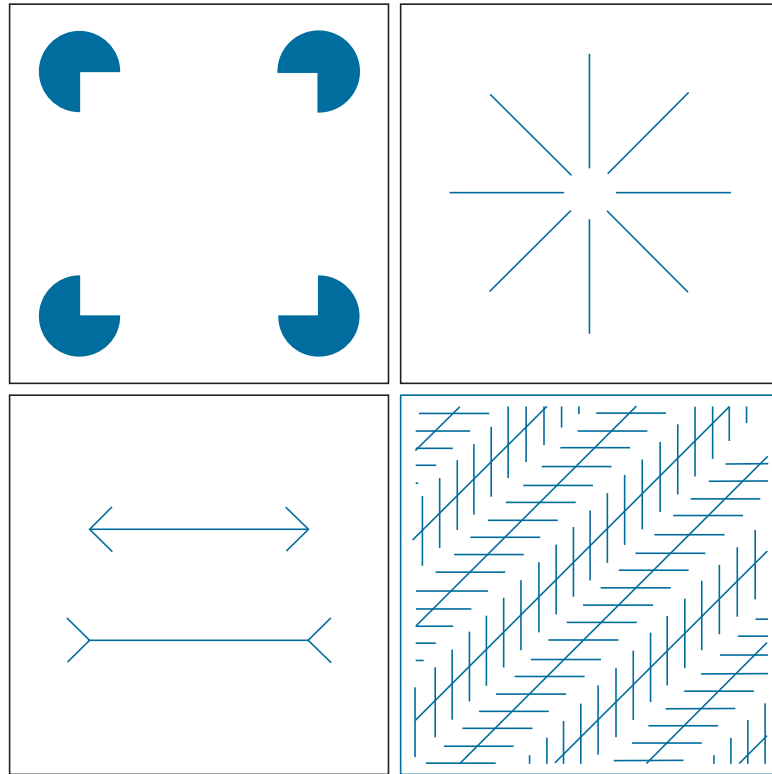
The electromagnetic spectrum can be expressed in terms of wavelength, frequency, or energy. Wavelength (λ) and frequency (ν) are related by the expression

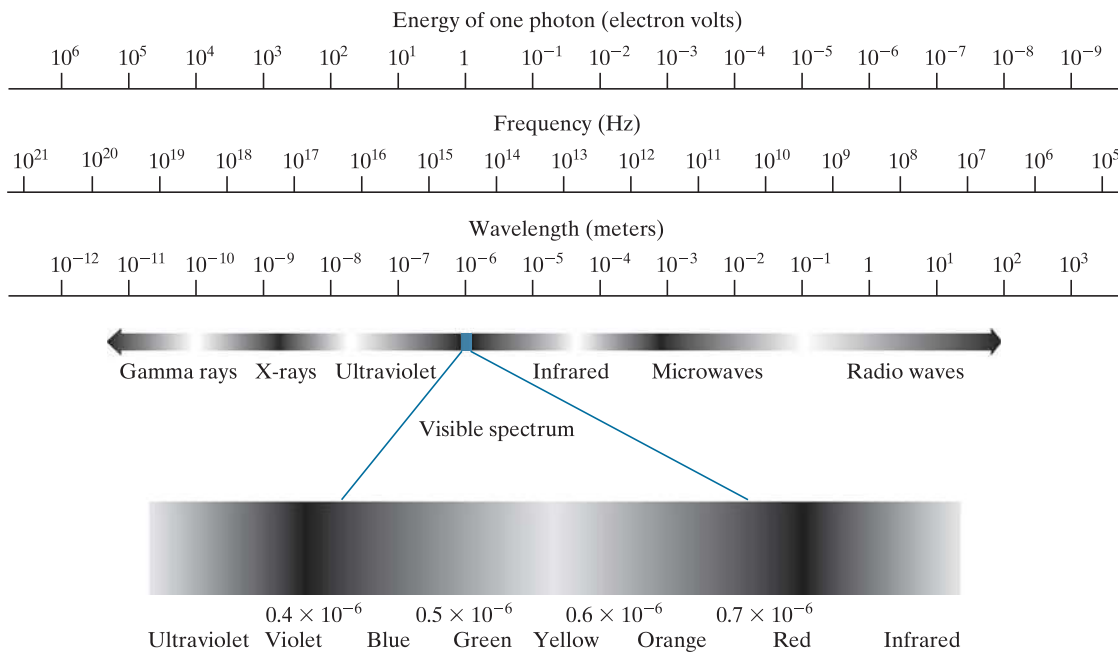$$\lambda = \frac{c}{\nu} \qquad (2\text{-}1)$$

where c is the speed of light (2.998×10^{8} m/s). Figure 2.11 shows a schematic representation of one wavelength.

The energy of the various components of the electromagnetic spectrum is given by the expression

$$E = h\nu \qquad (2\text{-}2)$$

where h is Planck's constant. The units of wavelength are meters, with the terms *microns* (denoted μm and equal to 10^{-6} m) and *nanometers* (denoted nm and equal to 10^{-9} m) being used just as frequently. Frequency is measured in *Hertz* (Hz), with one Hz being equal to one cycle of a sinusoidal wave per second. A commonly used unit of energy is the *electron-volt*.

Electromagnetic waves can be visualized as propagating sinusoidal waves with wavelength λ (Fig. 2.11), or they can be thought of as a stream of massless particles,

Energy of one photon (electron volts)

| 10^6 | 10^5 | 10^4 | 10^3 | 10^2 | 10^1 | 1 | 10^{-1} | 10^{-2} | 10^{-3} | 10^{-4} | 10^{-5} | 10^{-6} | 10^{-7} | 10^{-8} | 10^{-9} |

Frequency (Hz)

| 10^{21} | 10^{20} | 10^{19} | 10^{18} | 10^{17} | 10^{16} | 10^{15} | 10^{14} | 10^{13} | 10^{12} | 10^{11} | 10^{10} | 10^9 | 10^8 | 10^7 | 10^6 | 10^5 |

Wavelength (meters)

| 10^{-12} | 10^{-11} | 10^{-10} | 10^{-9} | 10^{-8} | 10^{-7} | 10^{-6} | 10^{-5} | 10^{-4} | 10^{-3} | 10^{-2} | 10^{-1} | 1 | 10^1 | 10^2 | 10^3 |

Gamma rays   X-rays   Ultraviolet   Infrared   Microwaves   Radio waves

Visible spectrum

0.4×10^{-6} 0.5×10^{-6} 0.6×10^{-6} 0.7×10^{-6}

Ultraviolet   Violet   Blue   Green   Yellow   Orange   Red   Infrared

FIGURE 2.10 The electromagnetic spectrum. The visible spectrum is shown zoomed to facilitate explanations, but note that it encompasses a very narrow range of the total EM spectrum.

each traveling in a wavelike pattern and moving at the speed of light. Each mass-less particle contains a certain amount (or bundle) of energy, called a *photon*. We see from Eq. (2-2) that energy is proportional to frequency, so the higher-frequency (shorter wavelength) electromagnetic phenomena carry more energy per photon. Thus, radio waves have photons with low energies, microwaves have more energy than radio waves, infrared still more, then visible, ultraviolet, X-rays, and finally gamma rays, the most energetic of all. High-energy electromagnetic radiation, especially in the X-ray and gamma ray bands, is particularly harmful to living organisms.

Light is a type of electromagnetic radiation that can be sensed by the eye. The visible (color) spectrum is shown expanded in Fig. 2.10 for the purpose of discussion (we will discuss color in detail in Chapter 6). The visible band of the electromagnetic spectrum spans the range from approximately 0.43 μm (violet) to about 0.79 μm (red). For convenience, the color spectrum is divided into six broad regions: violet, blue, green, yellow, orange, and red. No color (or other component of the

FIGURE 2.11
Graphical
representation of
one wavelength.
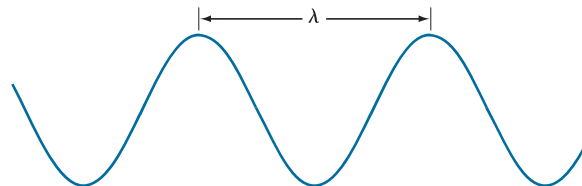
electromagnetic spectrum) ends abruptly; rather, each range blends smoothly into the next, as Fig. 2.10 shows.

The colors perceived in an object are determined by the nature of the light *reflected* by the object. A body that reflects light relatively balanced in all visible wavelengths appears white to the observer. However, a body that favors reflectance in a limited range of the visible spectrum exhibits some shades of color. For example, green objects reflect light with wavelengths primarily in the 500 to 570 nm range, while absorbing most of the energy at other wavelengths.

Light that is void of color is called *monochromatic* (or *achromatic*) light. The only attribute of monochromatic light is its intensity. Because the intensity of monochromatic light is perceived to vary from black to grays and finally to white, the term *gray level* is used commonly to denote monochromatic intensity (we use the terms *intensity* and *gray level* interchangeably in subsequent discussions). The range of values of monochromatic light from black to white is usually called the *gray scale*, and monochromatic images are frequently referred to as *grayscale images*.

Chromatic (color) light spans the electromagnetic energy spectrum from approximately 0.43 to 0.79 μm, as noted previously. In addition to frequency, three other quantities are used to describe a chromatic light source: radiance, luminance, and brightness. *Radiance* is the total amount of energy that flows from the light source, and it is usually measured in watts (W). *Luminance*, measured in lumens (lm), gives a measure of the amount of energy an observer *perceives* from a light source. For example, light emitted from a source operating in the far infrared region of the spectrum could have significant energy (radiance), but an observer would hardly perceive it; its luminance would be almost zero. Finally, as discussed in Section 2.1, *brightness* is a subjective descriptor of light perception that is practically impossible to measure. It embodies the achromatic notion of intensity and is one of the key factors in describing color sensation.

In principle, if a sensor can be developed that is capable of detecting energy radiated in a band of the electromagnetic spectrum, we can image events of interest in that band. Note, however, that the wavelength of an electromagnetic wave required to "see" an object must be of the same size as, or smaller than, the object. For example, a water molecule has a diameter on the order of 10^{-10} m. Thus, to study these molecules, we would need a source capable of emitting energy in the far (high-energy) ultraviolet band or soft (low-energy) X-ray bands.

Although imaging is based predominantly on energy from electromagnetic wave radiation, this is not the only method for generating images. For example, we saw in Section 1.3 that sound reflected from objects can be used to form ultrasonic images. Other sources of digital images are electron beams for electron microscopy, and software for generating synthetic images used in graphics and visualization.

2.3 IMAGE SENSING AND ACQUISITION

Most of the images in which we are interested are generated by the combination of an "illumination" source and the reflection or absorption of energy from that source by the elements of the "scene" being imaged. We enclose *illumination* and *scene* in quotes to emphasize the fact that they are considerably more general than the

familiar situation in which a visible light source illuminates a familiar 3-D scene. For example, the illumination may originate from a source of electromagnetic energy, such as a radar, infrared, or X-ray system. But, as noted earlier, it could originate from less traditional sources, such as ultrasound or even a computer-generated illumination pattern. Similarly, the scene elements could be familiar objects, but they can just as easily be molecules, buried rock formations, or a human brain. Depending on the nature of the source, illumination energy is reflected from, or transmitted through, objects. An example in the first category is light reflected from a planar surface. An example in the second category is when X-rays pass through a patient's body for the purpose of generating a diagnostic X-ray image. In some applications, the reflected or transmitted energy is focused onto a photo converter (e.g., a phosphor screen) that converts the energy into visible light. Electron microscopy and some applications of gamma imaging use this approach.

Figure 2.12 shows the three principal sensor arrangements used to transform incident energy into digital images. The idea is simple: Incoming energy is transformed into a voltage by a combination of the input electrical power and sensor material that is responsive to the type of energy being detected. The output voltage waveform is the response of the sensor, and a digital quantity is obtained by digitizing that response. In this section, we look at the principal modalities for image sensing and generation. We will discuss image digitizing in Section 2.4.

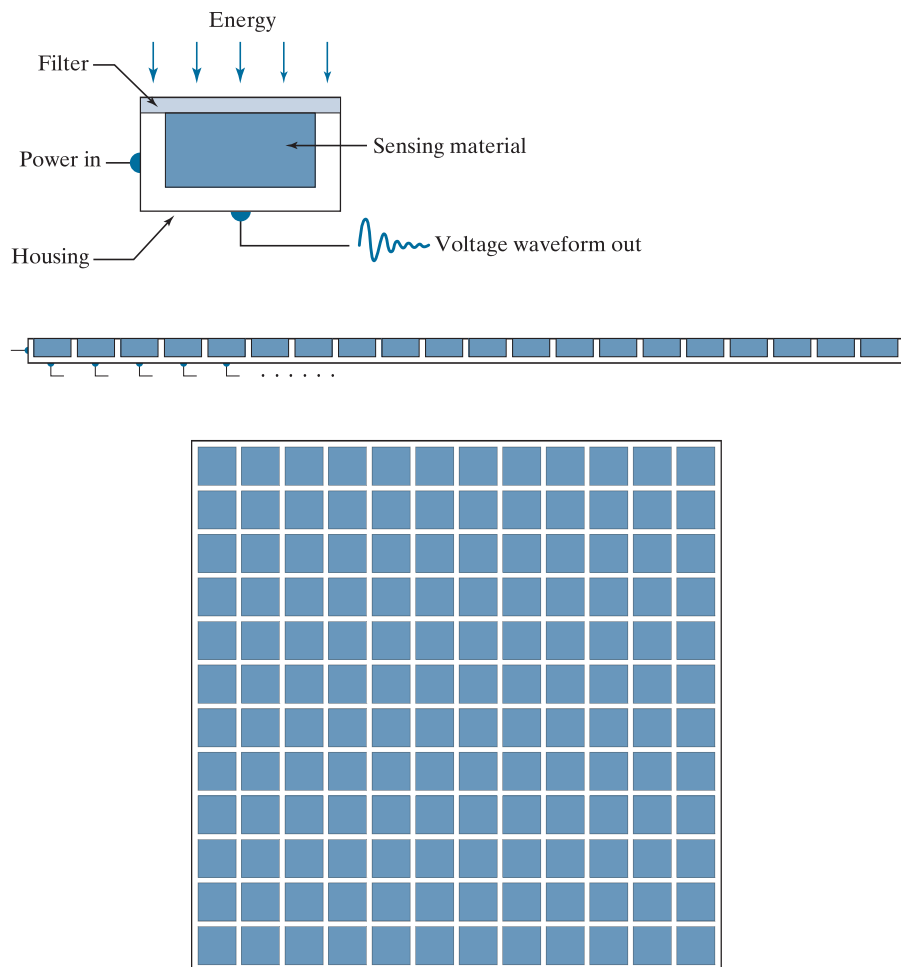## IMAGE ACQUISITION USING A SINGLE SENSING ELEMENT

Figure 2.12(a) shows the components of a single sensing element. A familiar sensor of this type is the photodiode, which is constructed of silicon materials and whose output is a voltage proportional to light intensity. Using a filter in front of a sensor improves its selectivity. For example, an optical green-transmission filter favors light in the green band of the color spectrum. As a consequence, the sensor output would be stronger for green light than for other visible light components.

In order to generate a 2-D image using a single sensing element, there has to be relative displacements in both the x- and y-directions between the sensor and the area to be imaged. Figure 2.13 shows an arrangement used in high-precision scanning, where a film negative is mounted onto a drum whose mechanical rotation provides displacement in one dimension. The sensor is mounted on a lead screw that provides motion in the perpendicular direction. A light source is contained inside the drum. As the light passes through the film, its intensity is modified by the film density before it is captured by the sensor. This "modulation" of the light intensity causes corresponding variations in the sensor voltage, which are ultimately converted to image intensity levels by digitization.
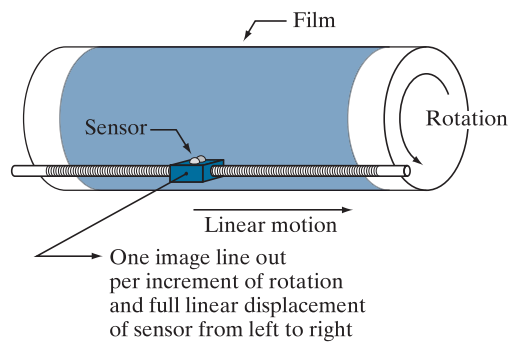
This method is an inexpensive way to obtain high-resolution images because mechanical motion can be controlled with high precision. The main disadvantages of this method are that it is slow and not readily portable. Other similar mechanical arrangements use a flat imaging bed, with the sensor moving in two linear directions. These types of mechanical digitizers sometimes are referred to as *transmission microdensitometers*. Systems in which light is reflected from the medium, instead of passing through it, are called *reflection microdensitometers*. Another example of imaging with a single sensing element places a laser source coincident with the

a
b
c

FIGURE 2.12
(a) Single sensing element.
(b) Line sensor.
(c) Array sensor.

Energy

Filter

Power in

Housing

Sensing material

Voltage waveform out

FIGURE 2.13
Combining a single sensing element with mechanical motion to generate a 2-D image.

Film

Sensor

Rotation

Linear motion

One image line out per increment of rotation and full linear displacement of sensor from left to right

sensor. Moving mirrors are used to control the outgoing beam in a scanning pattern and to direct the reflected laser signal onto the sensor.

## IMAGE ACQUISITION USING SENSOR STRIPS

A geometry used more frequently than single sensors is an in-line sensor strip, as in Fig. 2.12(b). The strip provides imaging elements in one direction. Motion perpendicular to the strip provides imaging in the other direction, as shown in Fig. 2.14(a). This arrangement is used in most flat bed scanners. Sensing devices with 4000 or more in-line sensors are possible. In-line sensors are used routinely in airborne imaging applications, in which the imaging system is mounted on an aircraft that flies at a constant altitude and speed over the geographical area to be imaged. One-dimensional imaging sensor strips that respond to various bands of the electromagnetic spectrum are mounted perpendicular to the direction of flight. An imaging strip gives one line of an image at a time, and the motion of the strip relative to the scene completes the other dimension of a 2-D image. Lenses or other focusing schemes are used to project the area to be scanned onto the sensors.

Sensor strips in a ring configuration are used in medical and industrial imaging to obtain cross-sectional ("slice") images of 3-D objects, as Fig. 2.14(b) shows. A rotating X-ray source provides illumination, and X-ray sensitive sensors opposite the source collect the energy that passes through the object. This is the basis for medical and industrial computerized axial tomography (CAT) imaging, as indicated in Sections 1.2 and 1.3. The output of the sensors is processed by reconstruction algorithms whose objective is to transform the sensed data into meaningful cross-sectional images (see Section 5.11). In other words, images are not obtained directly

a b

FIGURE 2.14
(a) Image acquisition using a linear sensor strip. (b) Image acquisition using a circular sensor strip.
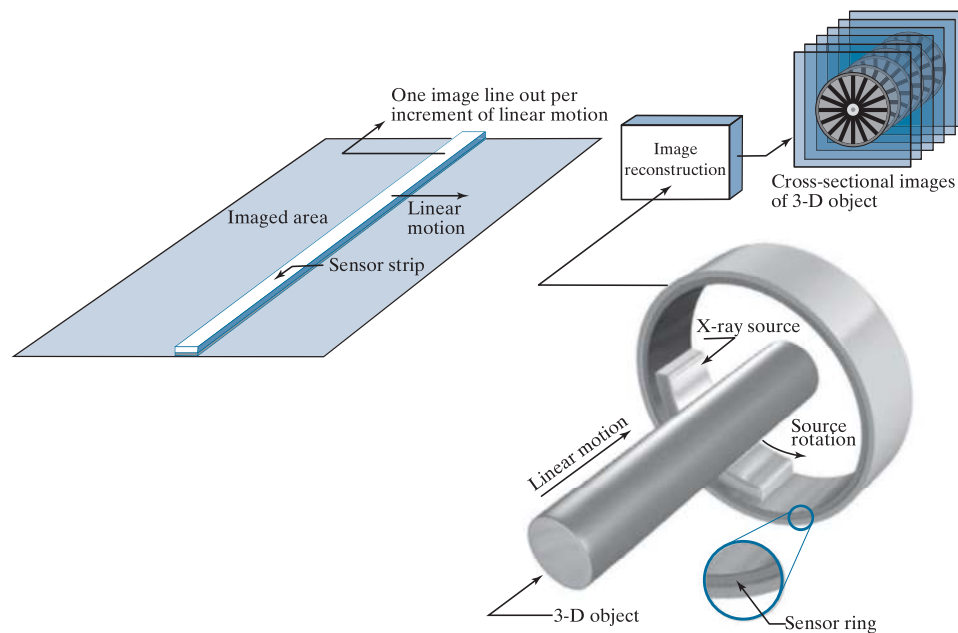
from the sensors by motion alone; they also require extensive computer processing. A 3-D digital volume consisting of stacked images is generated as the object is moved in a direction perpendicular to the sensor ring. Other modalities of imaging based on the CAT principle include magnetic resonance imaging (MRI) and positron emission tomography (PET). The illumination sources, sensors, and types of images are different, but conceptually their applications are very similar to the basic imaging approach shown in Fig. 2.14(b).

IMAGE ACQUISITION USING SENSOR ARRAYS

Figure 2.12(c) shows individual sensing elements arranged in the form of a 2-D array. Electromagnetic and ultrasonic sensing devices frequently are arranged in this manner. This is also the predominant arrangement found in digital cameras. A typical sensor for these cameras is a CCD (charge-coupled device) array, which can be manufactured with a broad range of sensing properties and can be packaged in rugged arrays of 4000×4000 elements or more. CCD sensors are used widely in digital cameras and other light-sensing instruments. The response of each sensor is proportional to the integral of the light energy projected onto the surface of the sensor, a property that is used in astronomical and other applications requiring low noise images. Noise reduction is achieved by letting the sensor integrate the input light signal over minutes or even hours. Because the sensor array in Fig. 2.12(c) is two-dimensional, its key advantage is that a complete image can be obtained by focusing the energy pattern onto the surface of the array. Motion obviously is not necessary, as is the case with the sensor arrangements discussed in the preceding two sections.

In some cases, the source is imaged directly, as in obtaining images of the sun.

Figure 2.15 shows the principal manner in which array sensors are used. This figure shows the energy from an illumination source being reflected from a scene (as mentioned at the beginning of this section, the energy also could be transmitted through the scene). The first function performed by the imaging system in Fig. 2.15(c) is to collect the incoming energy and focus it onto an image plane. If the illumination is light, the front end of the imaging system is an optical lens that projects the viewed scene onto the focal plane of the lens, as Fig. 2.15(d) shows. The sensor array, which is coincident with the focal plane, produces outputs proportional to the integral of the light received at each sensor. Digital and analog circuitry sweep these outputs and convert them to an analog signal, which is then digitized by another section of the imaging system. The output is a digital image, as shown diagrammatically in Fig. 2.15(e). Converting images into digital form is the topic of Section 2.4.

A SIMPLE IMAGE FORMATION MODEL

As introduced in Section 1.1, we denote images by two-dimensional functions of the form $f(x, y)$. The value of f at spatial coordinates (x, y) is a scalar quantity whose physical meaning is determined by the source of the image, and whose values are proportional to energy radiated by a physical source (e.g., electromagnetic waves). As a consequence, $f(x, y)$ must be nonnegative[†] and finite; that is,

---

[†] Image intensities can become negative during processing, or as a result of interpretation. For example, in radar images, objects moving toward the radar often are interpreted as having negative velocities while objects moving away are interpreted as having positive velocities. Thus, a velocity image might be coded as having both positive and negative values. When storing and displaying images, we normally scale the intensities so that the smallest negative value becomes 0 (see Section 2.6 regarding intensity scaling).

a
b c d e
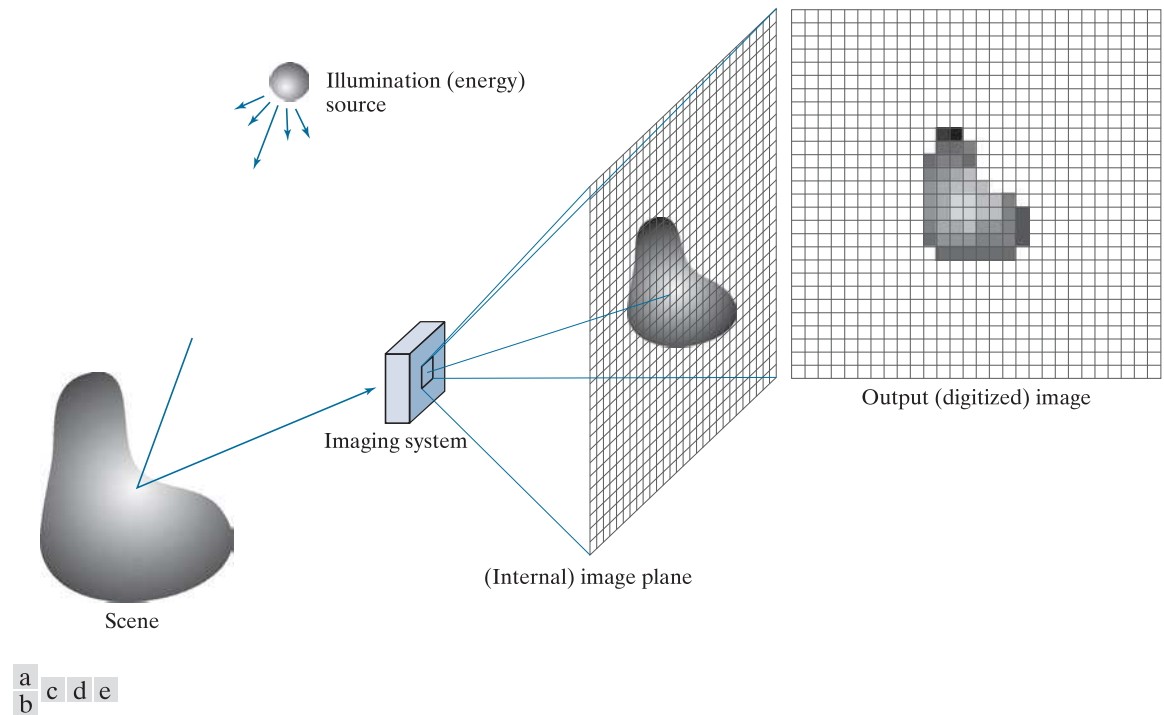
FIGURE 2.15 An example of digital image acquisition. (a) Illumination (energy) source. (b) A scene. (c) Imaging system. (d) Projection of the scene onto the image plane. (e) Digitized image.

$$0 \le f(x, y) < \infty \tag{2-3}$$

Function $f(x, y)$ is characterized by two components: (1) the amount of source illumination incident on the scene being viewed, and (2) the amount of illumination reflected by the objects in the scene. Appropriately, these are called the *illumination* and *reflectance* components, and are denoted by $i(x, y)$ and $r(x, y)$, respectively. The two functions combine as a product to form $f(x, y)$:

$$f(x, y) = i(x, y) r(x, y) \tag{2-4}$$

where

$$0 \le i(x, y) < \infty \tag{2-5}$$

and

$$0 \le r(x, y) \le 1 \tag{2-6}$$

Thus, reflectance is bounded by 0 (total absorption) and 1 (total reflectance). The nature of $i(x, y)$ is determined by the illumination source, and $r(x, y)$ is determined by the characteristics of the imaged objects. These expressions are applicable also to images formed via transmission of the illumination through a medium, such as a

chest X-ray. In this case, we would deal with a *transmissivity* instead of a *reflectivity* function, but the limits would be the same as in Eq. (2-6), and the image function formed would be modeled as the product in Eq. (2-4).

EXAMPLE 2.1: Some typical values of illumination and reflectance.

The following numerical quantities illustrate some typical values of illumination and reflectance for visible light. On a clear day, the sun may produce in excess of $90,000$ lm/m^2 of illumination on the surface of the earth. This value decreases to less than $10,000$ lm/m^2 on a cloudy day. On a clear evening, a full moon yields about 0.1 lm/m^2 of illumination. The typical illumination level in a commercial office is about $1,000$ lm/m^2. Similarly, the following are typical values of $r(x,y)$: 0.01 for black velvet, 0.65 for stainless steel, 0.80 for flat-white wall paint, 0.90 for silver-plated metal, and 0.93 for snow.

Let the intensity (gray level) of a monochrome image at any coordinates (x,y) be denoted by

$$\ell = f(x,y) \qquad (2\text{-}7)$$

From Eqs. (2-4) through (2-6) it is evident that ℓ lies in the range

$$L_{\min} \leq \ell \leq L_{\max} \qquad (2\text{-}8)$$

In theory, the requirement on $L_{\min}$ is that it be nonnegative, and on $L_{\max}$ that it be finite. In practice, $L_{\min} = i_{\min}r_{\min}$ and $L_{\max} = i_{\max}r_{\max}$. From Example 2.1, using average office illumination and reflectance values as guidelines, we may expect $L_{\min} \approx 10$ and $L_{\max} \approx 1000$ to be typical indoor values in the absence of additional illumination. The units of these quantities are lum/m^2. However, actual units seldom are of interest, except in cases where photometric measurements are being performed.

The interval $[L_{\min}, L_{\max}]$ is called the *intensity* (or *gray*) *scale*. Common practice is to shift this interval numerically to the interval $[0,1]$, or $[0,C]$, where $\ell = 0$ is considered black and $\ell = 1$ (or C) is considered white on the scale. All intermediate values are shades of gray varying from black to white.

2.4 IMAGE SAMPLING AND QUANTIZATION

The discussion of sampling in this section is of an intuitive nature. We will discuss this topic in depth in Chapter 4.

As discussed in the previous section, there are numerous ways to acquire images, but our objective in all is the same: to generate digital images from sensed data. The output of most sensors is a continuous voltage waveform whose amplitude and spatial behavior are related to the physical phenomenon being sensed. To create a digital image, we need to convert the continuous sensed data into a digital format. This requires two processes: *sampling* and *quantization*.

### BASIC CONCEPTS IN SAMPLING AND QUANTIZATION

Figure 2.16(a) shows a continuous image f that we want to convert to digital form. An image may be continuous with respect to the x- and y-coordinates, and also in

a b
c d

FIGURE 2.16
(a) Continuous
image. (b) A
scan line show-
ing intensity
variations along
line AB in the
continuous image.
(c) Sampling and
quantization.
(d) Digital scan
line. (The black
border in (a) is
included for
clarity. It is not
part of the image).
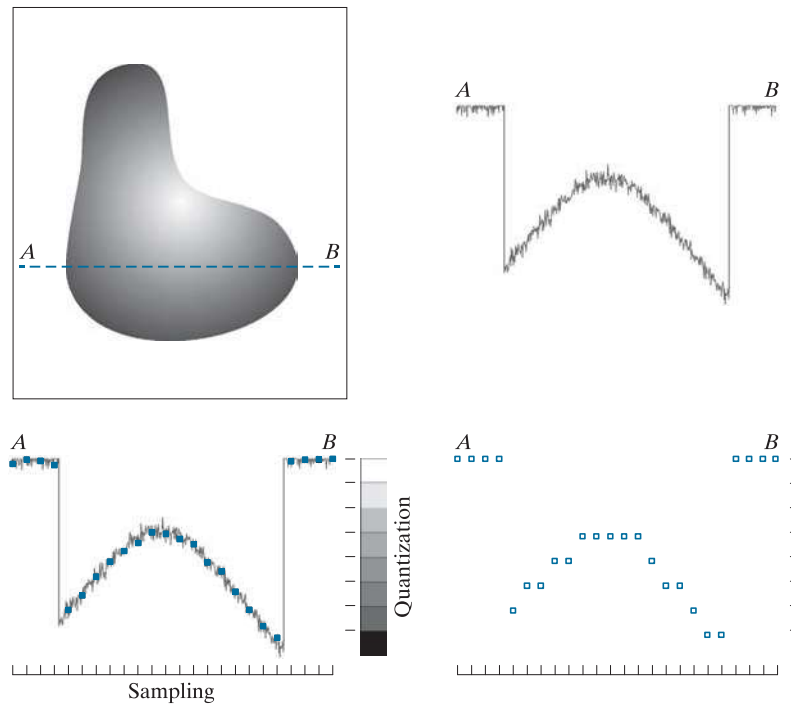
amplitude. To digitize it, we have to sample the function in both coordinates and also in amplitude. Digitizing the coordinate values is called *sampling*. Digitizing the amplitude values is called *quantization*.

The one-dimensional function in Fig. 2.16(b) is a plot of amplitude (intensity level) values of the continuous image along the line segment AB in Fig. 2.16(a). The random variations are due to image noise. To sample this function, we take equally spaced samples along line AB, as shown in Fig. 2.16(c). The samples are shown as small dark squares superimposed on the function, and their (discrete) spatial locations are indicated by corresponding tick marks in the bottom of the figure. The set of dark squares constitute the *sampled* function. However, the *values* of the samples still span (vertically) a continuous range of intensity values. In order to form a digital function, the intensity values also must be converted (*quantized*) into *discrete* quantities. The vertical gray bar in Fig. 2.16(c) depicts the intensity scale divided into eight discrete intervals, ranging from black to white. The vertical tick marks indicate the specific value assigned to each of the eight intensity intervals. The continuous intensity levels are quantized by assigning one of the eight values to each sample, depending on the vertical proximity of a sample to a vertical tick mark. The digital samples resulting from both sampling and quantization are shown as white squares in Fig. 2.16(d). Starting at the top of the continuous image and carrying out this procedure downward, line by line, produces a two-dimensional digital image. It is implied in Fig. 2.16 that, in addition to the number of discrete levels used, the accuracy achieved in quantization is highly dependent on the noise content of the sampled signal.

a b

FIGURE 2.17
(a) Continuous
image projected
onto a sensor
array. (b) Result
of image sampling
and quantization.
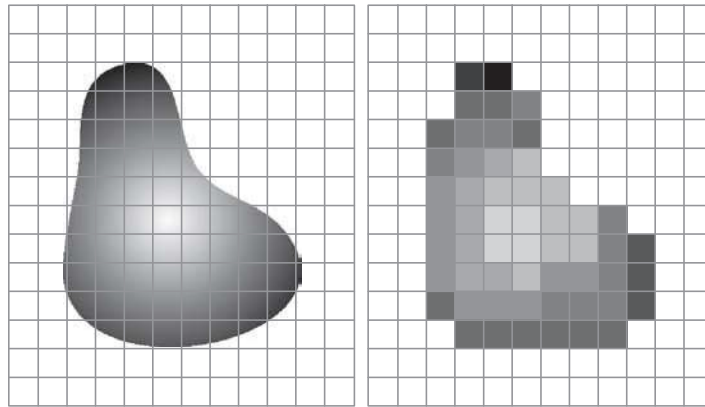
In practice, the method of sampling is determined by the sensor arrangement used to generate the image. When an image is generated by a single sensing element combined with mechanical motion, as in Fig. 2.13, the output of the sensor is quantized in the manner described above. However, spatial sampling is accomplished by selecting the number of individual mechanical increments at which we activate the sensor to collect data. Mechanical motion can be very exact so, in principle, there is almost no limit on how fine we can sample an image using this approach. In practice, limits on sampling accuracy are determined by other factors, such as the quality of the optical components used in the system.

When a sensing strip is used for image acquisition, the number of sensors in the strip establishes the samples in the resulting image in one direction, and mechanical motion establishes the number of samples in the other. Quantization of the sensor outputs completes the process of generating a digital image.

When a sensing array is used for image acquisition, no motion is required. The number of sensors in the array establishes the limits of sampling in both directions. Quantization of the sensor outputs is as explained above. Figure 2.17 illustrates this concept. Figure 2.17(a) shows a continuous image projected onto the plane of a 2-D sensor. Figure 2.17(b) shows the image after sampling and quantization. The quality of a digital image is determined to a large degree by the number of samples and discrete intensity levels used in sampling and quantization. However, as we will show later in this section, image content also plays a role in the choice of these parameters.

REPRESENTING DIGITAL IMAGES

Let $f(s,t)$ represent a *continuous* image function of two continuous variables, s and t. We convert this function into a *digital image* by sampling and quantization, as explained in the previous section. Suppose that we sample the continuous image into a digital image, $f(x,y)$, containing M rows and N columns, where (x,y) are discrete coordinates. For notational clarity and convenience, we use integer values for these discrete coordinates: $x = 0, 1, 2, \ldots, M-1$ and $y = 0, 1, 2, \ldots, N-1$. Thus, for example, the value of the digital image at the origin is $f(0,0)$, and its value at the next coordinates along the first row is $f(0,1)$. Here, the notation $(0, 1)$ is used

to denote the second sample along the first row. It *does not* mean that these are the values of the physical coordinates when the image was sampled. In general, the value of a digital image at any coordinates (x, y) is denoted $f(x, y)$, where x and y are integers. When we need to refer to specific coordinates (i, j), we use the notation $f(i, j)$, where the arguments are integers. The section of the real plane spanned by the coordinates of an image is called the *spatial domain*, with x and y being referred to as *spatial variables* or *spatial coordinates*.

Figure 2.18 shows three ways of representing $f(x, y)$. Figure 2.18(a) is a plot of the function, with two axes determining spatial location and the third axis being the values of f as a function of x and y. This representation is useful when working with grayscale sets whose elements are expressed as triplets of the form (x, y, z), where x and y are spatial coordinates and z is the value of f at coordinates (x, y). We will work with this representation briefly in Section 2.6.

The representation in Fig. 2.18(b) is more common, and it shows $f(x, y)$ as it would appear on a computer display or photograph. Here, the intensity of each point in the display is proportional to the value of f at that point. In this figure, there are only three equally spaced intensity values. If the intensity is normalized to the interval $[0, 1]$, then each point in the image has the value 0, 0.5, or 1. A monitor or printer converts these three values to black, gray, or white, respectively, as in Fig. 2.18(b). This type of representation includes color images, and allows us to view results at a glance.

As Fig. 2.18(c) shows, the third representation is an array (matrix) composed of the numerical values of $f(x, y)$. This is the representation used for computer processing. In equation form, we write the representation of an $M \times N$ numerical array as

$$f(x, y) = \begin{bmatrix} f(0,0) & f(0,1) & \cdots & f(0, N-1) \\ f(1,0) & f(1,1) & \cdots & f(1, N-1) \\ \vdots & \vdots & & \vdots \\ f(M-1,0) & f(M-1,1) & \cdots & f(M-1, N-1) \end{bmatrix} \tag{2-9}$$

The right side of this equation is a digital image represented as an array of real numbers. Each element of this array is called an *image element*, *picture element*, *pixel*, or *pel*. We use the terms *image* and *pixel* throughout the book to denote a digital image and its elements. Figure 2.19 shows a graphical representation of an image array, where the x- and y-axis are used to denote the rows and columns of the array. Specific pixels are values of the array at a fixed pair of coordinates. As mentioned earlier, we generally use $f(i, j)$ when referring to a pixel with coordinates (i, j).

We can also represent a digital image in a traditional matrix form:
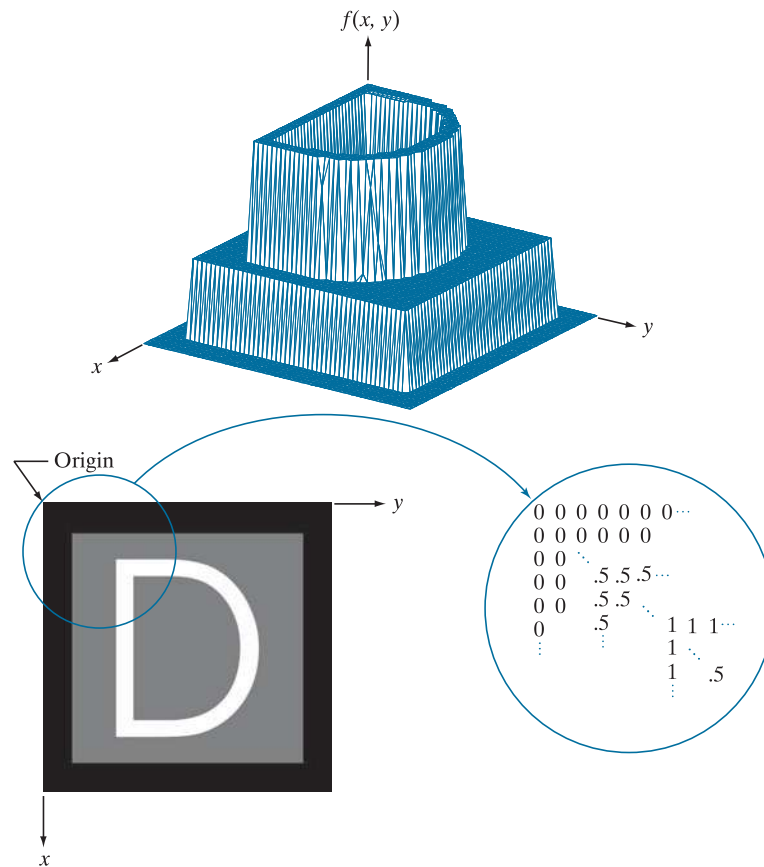
$$\mathbf{A} = \begin{bmatrix} a_{0,0} & a_{0,1} & \cdots & a_{0,N-1} \\ a_{1,0} & a_{1,1} & \cdots & a_{1,N-1} \\ \vdots & \vdots & & \vdots \\ a_{M-1,0} & a_{M-1,1} & \cdots & a_{M-1,N-1} \end{bmatrix} \tag{2-10}$$

Clearly, $a_{ij} = f(i, j)$, so Eqs. (2-9) and (2-10) denote identical arrays.

a
b c

FIGURE 2.18
(a) Image plotted
as a surface.
(b) Image displayed
as a visual intensity
array. (c) Image
shown as a 2-D nu-
merical array. (The
numbers 0, .5, and
1 represent black,
gray, and white,
respectively.)

As Fig. 2.19 shows, we define the *origin* of an image at the top left corner. This is a convention based on the fact that many image displays (e.g., TV monitors) sweep an image starting at the top left and moving to the right, one row at a time. More important is the fact that the first element of a matrix is by convention at the top left of the array. Choosing the origin of $f(x, y)$ at that point makes sense mathematically because digital images in reality are matrices. In fact, as you will see, sometimes we use x and y interchangeably in equations with the *rows* (r) and *columns* (c) of a matrix.

It is important to note that the representation in Fig. 2.19, in which the positive x-axis extends downward and the positive y-axis extends to the right, is precisely the right-handed Cartesian coordinate system with which you are familiar,[†] but shown rotated by 90° so that the origin appears on the top, left.

[†]Recall that a right-handed coordinate system is such that, when the index of the right hand points in the direction of the positive x-axis and the middle finger points in the (perpendicular) direction of the positive y-axis, the thumb points up. As Figs. 2.18 and 2.19 show, this indeed is the case in our image coordinate system. In practice, you will also find implementations based on a left-handed system, in which the x- and y-axis are interchanged from the way we show them in Figs. 2.18 and 2.19. For example, MATLAB uses a left-handed system for image processing. Both systems are perfectly valid, provided they are used consistently.

FIGURE 2.19
Coordinate
convention used
to represent digital
images. Because
coordinate values
are integers, there
is a one-to-one
correspondence
between x and y
and the rows (r)
and columns (c) of
a matrix.
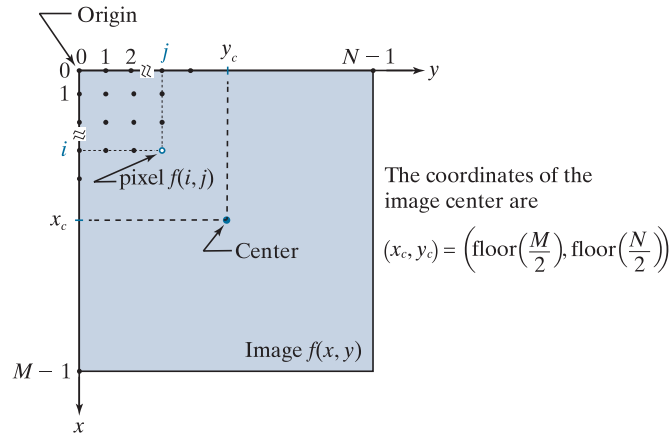
The *floor* of z, sometimes denoted $\lfloor z \rfloor$, is the largest integer that is less than or equal to z. The *ceiling* of z, denoted $\lceil z \rceil$, is the smallest integer that is greater than or equal to z.

The *center* of an $M \times N$ digital image with origin at $(0,0)$ and range to $(M - 1, N - 1)$ is obtained by dividing M and N by 2 and rounding *down* to the nearest integer. This operation sometimes is denoted using the floor operator, $\lfloor \cdot \rfloor$, as shown in Fig. 2.19. This holds true for M and N even *or* odd. For example, the center of an image of size 1023×1024 is at $(511, 512)$. Some programming languages (e.g., MATLAB) start indexing at 1 instead of at 0. The center of an image in that case is found at $(x_c, y_c) = (\text{floor}(M/2) + 1, \text{floor}(N/2) + 1)$.

To express sampling and quantization in more formal mathematical terms, let Z and R denote the set of integers and the set of real numbers, respectively. The sampling process may be viewed as partitioning the xy-plane into a grid, with the coordinates of the center of each cell in the grid being a pair of elements from the Cartesian product Z^2 (also denoted $Z \times Z$) which, as you may recall, is the set of all ordered pairs of elements (z_i, z_j) with z_i and z_j being integers from set Z. Hence, $f(x, y)$ is a digital image if (x, y) are integers from Z^2 and f is a function that assigns an intensity value (that is, a real number from the set of real numbers, R) to each distinct pair of coordinates (x, y). This functional assignment is the quantization process described earlier. If the intensity levels also are integers, then $R = Z$, and a digital image becomes a 2-D function whose coordinates and amplitude values are integers. This is the representation we use in the book.

See Eq. (2-41) in Section 2.6 for a formal definition of the Cartesian product.

Image digitization requires that decisions be made regarding the values for M, N, and for the number, L, of discrete intensity levels. There are no restrictions placed on M and N, other than they have to be positive integers. However, digital storage and quantizing hardware considerations usually lead to the number of intensity levels, L, being an integer power of two; that is

$$L = 2^k \tag{2-11}$$

where k is an integer. We assume that the discrete levels are equally spaced and that they are integers in the range $[0, L - 1]$.

FIGURE 2.20
An image exhibiting saturation and noise. Saturation is the highest value beyond which all intensity values are clipped (note how the entire saturated area has a high, constant intensity level). Visible noise in this case appears as a grainy texture pattern. The dark background is noisier, but the noise is difficult to see.
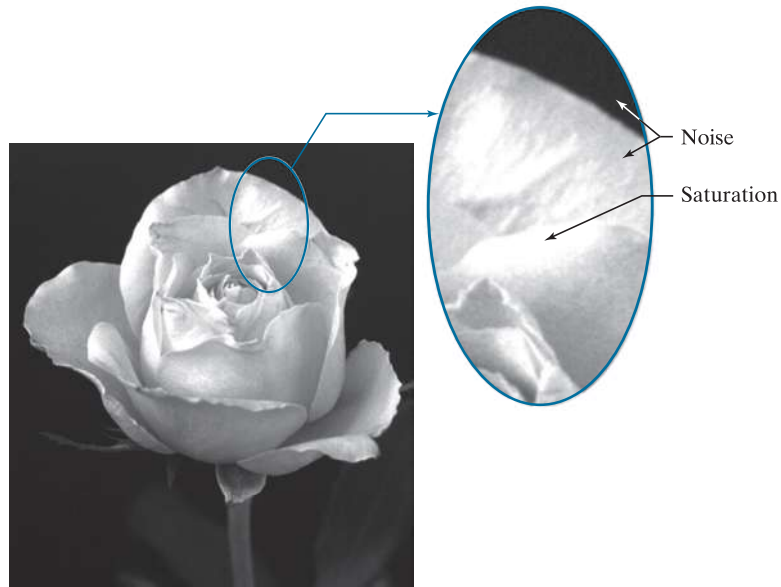
Sometimes, the range of values spanned by the gray scale is referred to as the *dynamic range*, a term used in different ways in different fields. Here, we define the dynamic range of an imaging system to be the ratio of the maximum measurable intensity to the minimum detectable intensity level in the system. As a rule, the upper limit is determined by *saturation* and the lower limit by *noise*, although noise can be present also in lighter intensities. Figure 2.20 shows examples of saturation and slight visible noise. Because the darker regions are composed primarily of pixels with the minimum detectable intensity, the background in Fig. 2.20 is the noisiest part of the image; however, dark background noise typically is much harder to see.

The dynamic range establishes the lowest and highest intensity levels that a system can represent and, consequently, that an image can have. Closely associated with this concept is *image contrast*, which we define as the difference in intensity between the highest and lowest intensity levels in an image. The *contrast ratio* is the ratio of these two quantities. When an appreciable number of pixels in an image have a high dynamic range, we can expect the image to have high contrast. Conversely, an image with low dynamic range typically has a dull, washed-out gray look. We will discuss these concepts in more detail in Chapter 3.

The number, b, of bits required to store a digital image is

$$b = M \times N \times k \qquad (2\text{-}12)$$

When $M = N$, this equation becomes

$$b = N^2 k \qquad (2\text{-}13)$$

FIGURE 2.21
Number of
megabytes
required to store
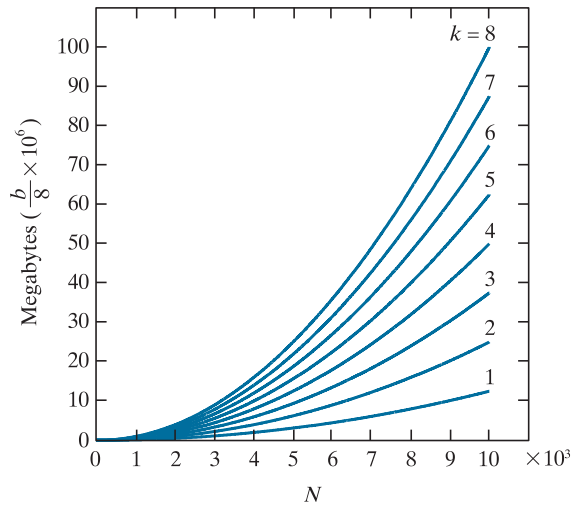images for
various values of
N and k.

Figure 2.21 shows the number of megabytes required to store square images for various values of N and k (as usual, one byte equals 8 bits and a megabyte equals 10^6 bytes).

When an image can have 2^k possible intensity levels, it is common practice to refer to it as a "k-bit image," (e,g., a 256-level image is called an *8-bit image*). Note that storage requirements for large 8-bit images (e.g., $10,000 \times 10,000$ pixels) are not insignificant.

LINEAR VS. COORDINATE INDEXING

The convention discussed in the previous section, in which the location of a pixel is given by its 2-D coordinates, is referred to as *coordinate indexing*, or *subscript indexing*. Another type of indexing used extensively in programming image processing algorithms is *linear indexing*, which consists of a 1-D string of nonnegative integers based on computing offsets from coordinates $(0,0)$. There are two principal types of linear indexing, one is based on a row scan of an image, and the other on a column scan.

Figure 2.22 illustrates the principle of linear indexing based on a column scan. The idea is to scan an image column by column, starting at the origin and proceeding down and then to the right. The linear index is based on counting pixels as we scan the image in the manner shown in Fig. 2.22. Thus, a scan of the first (leftmost) column yields linear indices 0 through $M - 1$. A scan of the second column yields indices M through $2M - 1$, and so on, until the last pixel in the last column is assigned the linear index value $MN - 1$. Thus, a linear index, denoted by α, has one of MN possible values: $0, 1, 2, \ldots, MN - 1$, as Fig. 2.22 shows. The important thing to notice here is that each pixel is assigned a linear index value that identifies it uniquely.

The formula for generating linear indices based on a column scan is straightforward and can be determined by inspection. For any pair of coordinates (x, y), the corresponding linear index value is

$$\alpha = My + x \tag{2-14}$$

FIGURE 2.22
Illustration of
column scanning
for generating
linear indices.
Shown are several
2-D coordinates (in
parentheses) and
their corresponding
linear indices.
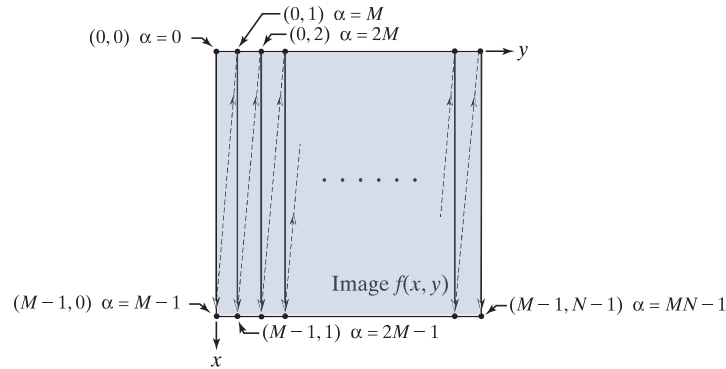
Conversely, the coordinate indices for a given linear index value α are given by the equations[†]

$$x = \alpha \bmod M \qquad (2\text{-}15)$$

and

$$y = (\alpha - x)/M \qquad (2\text{-}16)$$

Recall that $\alpha \bmod M$ means "the remainder of the division of α by M." This is a formal way of stating that row numbers repeat themselves at the start of every column. Thus, when $\alpha = 0$, the remainder of the division of 0 by M is 0, so $x = 0$. When $\alpha = 1$, the remainder is 1, and so $x = 1$. You can see that x will continue to be equal to α until $\alpha = M - 1$. When $\alpha = M$ (which is at the beginning of the second column), the remainder is 0, and thus $x = 0$ again, and it increases by 1 until the next column is reached, when the pattern repeats itself. Similar comments apply to Eq. (2-16). See Problem 2.11 for a derivation of the preceding two equations.

SPATIAL AND INTENSITY RESOLUTION

Intuitively, *spatial resolution* is a measure of the smallest discernible detail in an image. Quantitatively, spatial resolution can be stated in several ways, with *line pairs per unit distance*, and *dots (pixels) per unit distance* being common measures. Suppose that we construct a chart with alternating black and white vertical lines, each of width W units (W can be less than 1). The width of a *line pair* is thus $2W$, and there are $W/2$ line pairs per unit distance. For example, if the width of a line is 0.1 mm, there are 5 line pairs per unit distance (i.e., per mm). A widely used definition of image resolution is the largest number of *discernible* line pairs per unit distance (e.g., 100 line pairs per mm). Dots per unit distance is a measure of image resolution used in the printing and publishing industry. In the U.S., this measure usually is expressed as *dots per inch* (dpi). To give you an idea of quality, newspapers are printed with a

[†]When working with modular number systems, it is more accurate to write $x \equiv \alpha \bmod M$, where the symbol $\equiv$ means *congruence*. However, our interest here is just on converting from linear to coordinate indexing, so we use the more familiar equal sign.

resolution of 75 dpi, magazines at 133 dpi, glossy brochures at 175 dpi, and the book page at which you are presently looking was printed at 2400 dpi.

To be meaningful, measures of spatial resolution must be stated with respect to spatial units. Image size by itself does not tell the complete story. For example, to say that an image has a resolution of 1024×1024 pixels is not a meaningful statement without stating the spatial dimensions encompassed by the image. Size by itself is helpful only in making comparisons between imaging capabilities. For instance, a digital camera with a 20-megapixel CCD imaging chip can be expected to have a higher capability to resolve detail than an 8-megapixel camera, assuming that both cameras are equipped with comparable lenses and the comparison images are taken at the same distance.

Intensity resolution similarly refers to the smallest *discernible* change in intensity level. We have considerable discretion regarding the number of spatial samples (pixels) used to generate a digital image, but this is not true regarding the number of intensity levels. Based on hardware considerations, the number of intensity levels usually is an integer power of two, as we mentioned when discussing Eq. (2-11). The most common number is 8 bits, with 16 bits being used in some applications in which enhancement of specific intensity ranges is necessary. Intensity quantization using 32 bits is rare. Sometimes one finds systems that can digitize the intensity levels of an image using 10 or 12 bits, but these are not as common.

Unlike spatial resolution, which must be based on a per-unit-of-distance basis to be meaningful, it is common practice to refer to the number of bits used to quantize intensity as the "*intensity resolution*." For example, it is common to say that an image whose intensity is quantized into 256 levels has 8 bits of intensity resolution. However, keep in mind that *discernible* changes in intensity are influenced also by noise and saturation values, and by the capabilities of human perception to analyze and interpret details in the context of an entire scene (see Section 2.1). The following two examples illustrate the effects of spatial and intensity resolution on discernible detail. Later in this section, we will discuss how these two parameters interact in determining perceived image quality.

EXAMPLE 2.2: Effects of reducing the spatial resolution of a digital image.

Figure 2.23 shows the effects of reducing the spatial resolution of an image. The images in Figs. 2.23(a) through (d) have resolutions of 930, 300, 150, and 72 dpi, respectively. Naturally, the lower resolution images are smaller than the original image in (a). For example, the original image is of size 2136×2140 pixels, but the 72 dpi image is an array of only 165×166 pixels. In order to facilitate comparisons, all the smaller images were zoomed back to the original size (the method used for zooming will be discussed later in this section). This is somewhat equivalent to "getting closer" to the smaller images so that we can make comparable statements about visible details.

There are some small visual differences between Figs. 2.23(a) and (b), the most notable being a slight distortion in the seconds marker pointing to 60 on the right side of the chronometer. For the most part, however, Fig. 2.23(b) is quite acceptable. In fact, 300 dpi is the typical minimum image spatial resolution used for book publishing, so one would not expect to see much difference between these two images. Figure 2.23(c) begins to show visible degradation (see, for example, the outer edges of the chronometer

a b
c d

FIGURE 2.23
Effects of
reducing spatial
resolution. The
images shown
are at:
(a) 930 dpi,
(b) 300 dpi,
(c) 150 dpi, and
(d) 72 dpi.
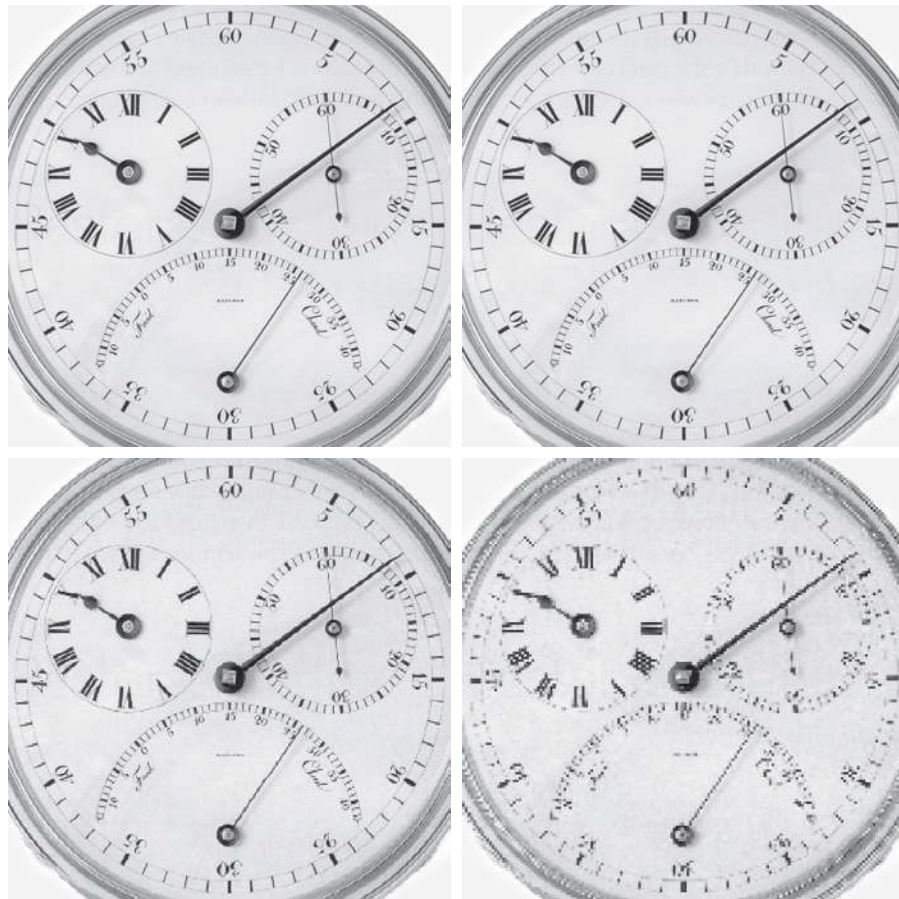
case and compare the seconds marker with the previous two images). The numbers also show visible degradation. Figure 2.23(d) shows degradation that is visible in most features of the image. When printing at such low resolutions, the printing and publishing industry uses a number of techniques (such as locally varying the pixel size) to produce much better results than those in Fig. 2.23(d). Also, as we will show later in this section, it is possible to improve on the results of Fig. 2.23 by the choice of interpolation method used.

EXAMPLE 2.3: Effects of varying the number of intensity levels in a digital image.

Figure 2.24(a) is a 774×640 CT projection image, displayed using 256 intensity levels (see Chapter 1 regarding CT images). The objective of this example is to reduce the number of intensities of the image from 256 to 2 in integer powers of 2, while keeping the spatial resolution constant. Figures 2.24(b) through (d) were obtained by reducing the number of intensity levels to 128, 64, and 32, respectively (we will discuss in Chapter 3 how to reduce the number of levels).

a b
c d

FIGURE 2.24
(a) 774×640, 256-level image. (b)-(d) Image displayed in 128, 64, and 32 intensity levels, while keeping the spatial resolution constant. (Original image courtesy of the Dr. David R. Pickens, Department of Radiology & Radiological Sciences, Vanderbilt University Medical Center.)
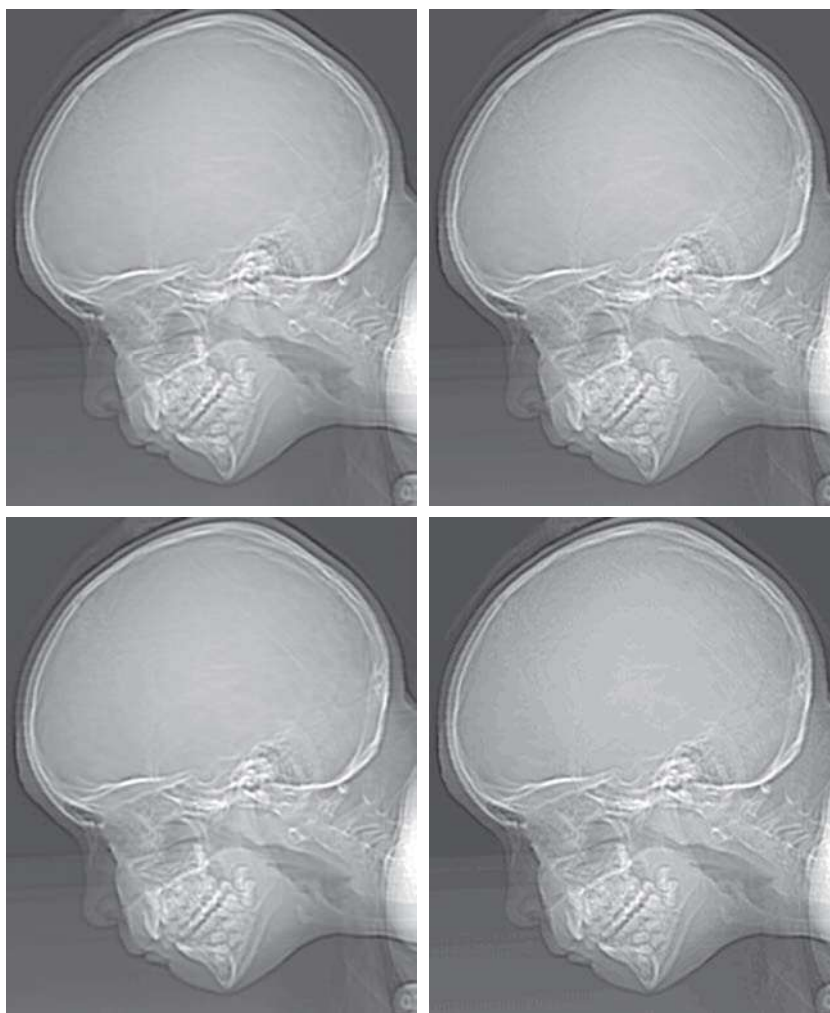

The 128- and 64-level images are visually identical for all practical purposes. However, the 32-level image in Fig. 2.24(d) has a set of almost imperceptible, very fine ridge-like structures in areas of constant intensity. These structures are clearly visible in the 16-level image in Fig. 2.24(e). This effect, caused by using an insufficient number of intensity levels in smooth areas of a digital image, is called *false contouring*, so named because the ridges resemble topographic contours in a map. False contouring generally is quite objectionable in images displayed using 16 or fewer uniformly spaced intensity levels, as the images in Figs. 2.24(e)-(h) show.

As a very rough guideline, and assuming integer powers of 2 for convenience, images of size 256×256 pixels with 64 intensity levels, and printed on a size format on the order of 5×5 cm, are about the lowest spatial and intensity resolution images that can be expected to be reasonably free of objectionable sampling distortions and false contouring.

e f
g h

FIGURE 2.24
(*Continued*)
(e)-(h) Image
displayed in 16, 8,
4, and 2 intensity
levels.
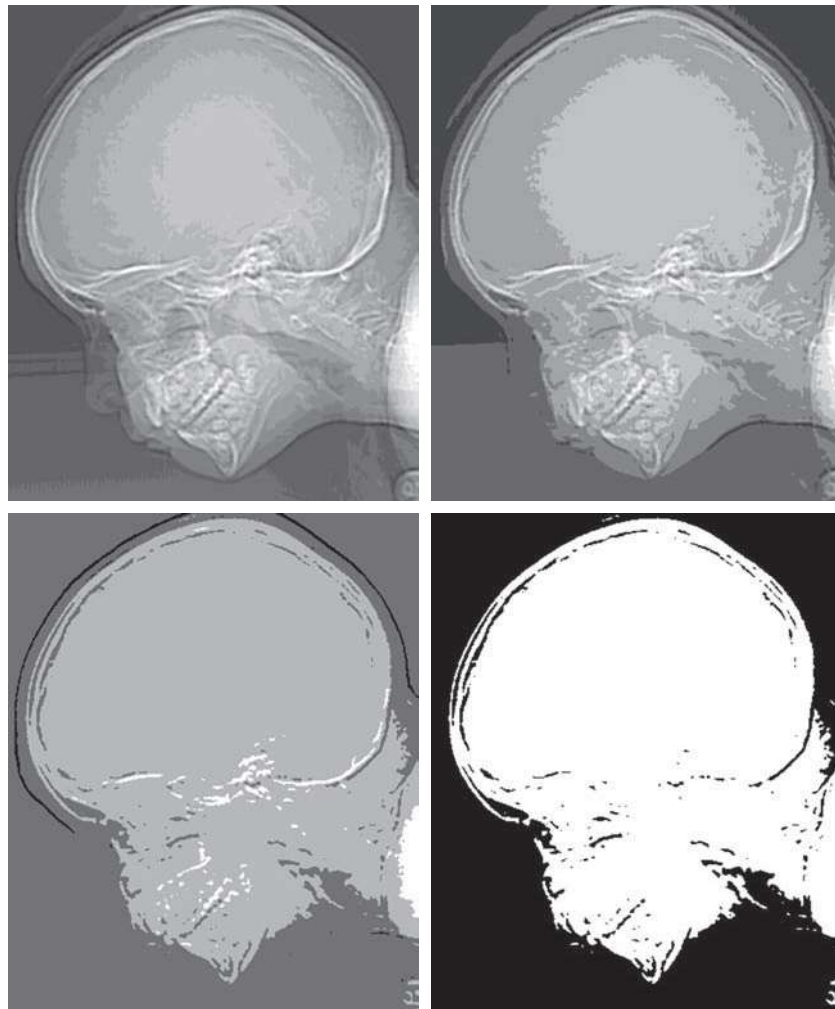
The results in Examples 2.2 and 2.3 illustrate the effects produced on image quality by varying spatial and intensity resolution independently. However, these results did not consider any relationships that might exist between these two parameters. An early study by Huang [1965] attempted to quantify experimentally the effects on image quality produced by the interaction of these two variables. The experiment consisted of a set of subjective tests. Images similar to those shown in Fig. 2.25 were used. The woman's face represents an image with relatively little detail; the picture of the cameraman contains an intermediate amount of detail; and the crowd picture contains, by comparison, a large amount of detail.

Sets of these three types of images of various sizes and intensity resolution were generated by varying N and k [see Eq. (2-13)]. Observers were then asked to rank

a b c

FIGURE 2.25 (a) Image with a low level of detail. (b) Image with a medium level of detail. (c) Image with a relatively large amount of detail. (Image (b) courtesy of the Massachusetts Institute of Technology.)

them according to their subjective quality. Results were summarized in the form of so-called *isopreference curves* in the Nk-plane. (Figure 2.26 shows average isopreference curves representative of the types of images in Fig. 2.25.) Each point in the Nk-plane represents an image having values of N and k equal to the coordinates of that point. Points lying on an isopreference curve correspond to images of equal subjective quality. It was found in the course of the experiments that the isopreference curves tended to shift right and upward, but their shapes in each of the three image categories were similar to those in Fig. 2.26. These results were not unexpected, because a shift up and right in the curves simply means larger values for N and k, which implies better picture quality.

FIGURE 2.26
Representative isopreference curves for the three types of images in Fig. 2.25.
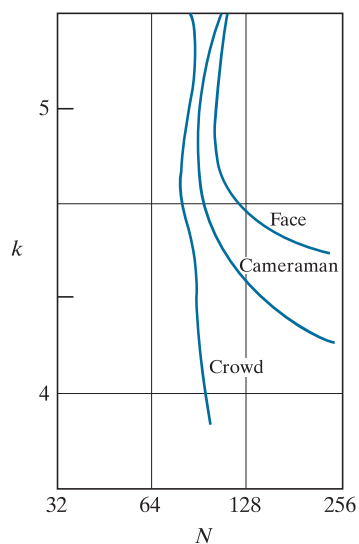
Observe that isopreference curves tend to become more vertical as the detail in the image increases. This result suggests that for images with a large amount of detail only a few intensity levels may be needed. For example, the isopreference curve in Fig. 2.26 corresponding to the crowd is nearly vertical. This indicates that, for a fixed value of N, the perceived quality for this type of image is nearly independent of the number of intensity levels used (for the range of intensity levels shown in Fig. 2.26). The perceived quality in the other two image categories remained the same in some intervals in which the number of samples was increased, but the number of intensity levels actually decreased. The most likely reason for this result is that a decrease in k tends to increase the apparent contrast, a visual effect often perceived as improved image quality.

IMAGE INTERPOLATION

Interpolation is used in tasks such as zooming, shrinking, rotating, and geometrically correcting digital images. Our principal objective in this section is to introduce interpolation and apply it to image resizing (shrinking and zooming), which are basically image resampling methods. Uses of interpolation in applications such as rotation and geometric corrections will be discussed in Section 2.6.

Interpolation is the process of using known data to estimate values at unknown locations. We begin the discussion of this topic with a short example. Suppose that an image of size 500×500 pixels has to be enlarged 1.5 times to 750×750 pixels. A simple way to visualize zooming is to create an imaginary 750×750 grid with the same pixel spacing as the original image, then shrink it so that it exactly overlays the original image. Obviously, the pixel spacing in the shrunken 750×750 grid will be less than the pixel spacing in the original image. To assign an intensity value to any point in the overlay, we look for its closest pixel in the underlying original image and assign the intensity of that pixel to the new pixel in the 750×750 grid. When intensities have been assigned to all the points in the overlay grid, we expand it back to the specified size to obtain the resized image.

The method just discussed is called *nearest neighbor interpolation* because it assigns to each new location the intensity of its nearest neighbor in the original image (see Section 2.5 regarding neighborhoods). This approach is simple but, it has the tendency to produce undesirable artifacts, such as severe distortion of straight edges. A more suitable approach is *bilinear interpolation*, in which we use the four nearest neighbors to estimate the intensity at a given location. Let (x, y) denote the coordinates of the location to which we want to assign an intensity value (think of it as a point of the grid described previously), and let $v(x, y)$ denote that intensity value. For bilinear interpolation, the assigned value is obtained using the equation

Contrary to what the name suggests, bilinear interpolation is *not* a linear operation because it involves multiplication of coordinates (which is not a linear operation). See Eq. (2-17).

$$v(x, y) = ax + by + cxy + d \qquad (2\text{-}17)$$

where the four coefficients are determined from the four equations in four unknowns that can be written using the *four* nearest neighbors of point (x, y). Bilinear interpolation gives much better results than nearest neighbor interpolation, with a modest increase in computational burden.

The next level of complexity is *bicubic interpolation*, which involves the sixteen nearest neighbors of a point. The intensity value assigned to point (x, y) is obtained using the equation

$$v(x, y) = \sum_{i=0}^{3} \sum_{j=0}^{3} a_{ij} x^i y^j \qquad (2\text{-}18)$$

The sixteen coefficients are determined from the sixteen equations with sixteen unknowns that can be written using the sixteen nearest neighbors of point (x, y). Observe that Eq. (2-18) reduces in form to Eq. (2-17) if the limits of both summations in the former equation are 0 to 1. Generally, bicubic interpolation does a better job of preserving fine detail than its bilinear counterpart. Bicubic interpolation is the standard used in commercial image editing applications, such as Adobe Photoshop and Corel Photopaint.

Although images are displayed with integer coordinates, it is possible during processing to work with *subpixel accuracy* by increasing the size of the image using interpolation to "fill the gaps" between pixels in the original image.

EXAMPLE 2.4: Comparison of interpolation approaches for image shrinking and zooming.

Figure 2.27(a) is the same as Fig. 2.23(d), which was obtained by reducing the resolution of the 930 dpi image in Fig. 2.23(a) to 72 dpi (the size shrank from 2136×2140 to 165×166 pixels) and then zooming the reduced image back to its original size. To generate Fig. 2.23(d) we used nearest neighbor interpolation both to shrink and zoom the image. As noted earlier, the result in Fig. 2.27(a) is rather poor. Figures 2.27(b) and (c) are the results of repeating the same procedure but using, respectively, bilinear and bicubic interpolation for both shrinking and zooming. The result obtained by using bilinear interpolation is a significant improvement over nearest neighbor interpolation, but the resulting image is blurred slightly. Much sharper results can be obtained using bicubic interpolation, as Fig. 2.27(c) shows.

a b c

FIGURE 2.27 (a) Image reduced to 72 dpi and zoomed back to its original 930 dpi using nearest neighbor interpolation. This figure is the same as Fig. 2.23(d). (b) Image reduced to 72 dpi and zoomed using bilinear interpolation. (c) Same as (b) but using bicubic interpolation.